Russian Journal of Earth Sciences

New Constraints of Interior Fars Sedimentary Basin Analysis During Asmari Formation (Oligocene-Lower Miocene) Deposition, South Iran

Maryam Yarem Taghloo Sohrabi[1], Bahman Soleimani[*,2], Vahid Ahmadi[3], Dawood Jahani[1], Nader Kohansal Ghadimvand[1]

[1]Islamic Azad University, Northern Tehran Branch, Tehran, Iran
[2]Shahid Chamran University of Ahvaz, Ahvaz, Iran
[3]Islamic Azad University, Shiraz Branch, Shiraz, Iran
* **Correspondence to:** Prof. Bahman Soleimani, soleimani_b@scu.ac.ir.

Abstract: Interior Fars region is an important geological province of Zagros basin due to historical events. The present paper focused on the time span of the Asmari deposition (Oligo-Lower Miocene) in Fars area bounded by Kazerun and Nezamabad faults. The studied samples of Asmari Formation were collected from 3 different stratigraphic sections A, B and C. The area is discussed in view of microfacies variation, sequence stratigraphy and environmental factors such as diagenetic processes and sea level changes. Microscopic studies led to identification 13 carbonate facies in this area. The results showed that the Asmari Formation has been deposited in a carbonate shelf in 5 sedimentary sub-environments including open sea, bar, lagoon, shoal and tidal flat. Basin changes were also compared with global sea level changes. Sequential stratigraphic evidence showed that the Asmari Formation consists of two sedimentary sequences of third order. The unconformity in the lower boundary of Asmari Formation with Jahrom Formation in sections-B and C can be ascribed to the result of Pyrenean orogenic phase activity in this area. The Asmari Formation in this area has been undergone extensively by diagenetic processes. Micriticization, dolomitization, cementation, hematitization, stylolitization, neomorphism and dissolution are among the important and noteworthy of diagenetic processes. The intensity of each process is a function of facies characteristics (fabric control). Microfacies data and sea level changes curve in local (the area), regional and global scales revealed that these facies are more correlated to the local sea level variation than others. The present study resulted to new main points related to the Fars basin evolution. Reactivation of faults (such as Kazerun and Nezamabad), regional sea level changes and Alpine orogenic phases impact (i.e., Pyrenean phase) have involved a major role in sedimentary facies distribution and basin evolution.

Keywords: Asmari Formation, Interior Fars, Pyrenean phase, sea level changes.

Citation: Sohrabi, Maryam Yarem Taghloo, Bahman Soleimani, Vahid Ahmadi, Dawood Jahani, and Nader Kohansal Ghadimvand (2024), New Constraints of Interior Fars Sedimentary Basin Analysis During Asmari Formation (Oligocene-Lower Miocene) Deposition, South Iran, *Russian Journal of Earth Sciences*, 24, ES2005, EDN: SAJHWH, https://doi.org/10.2205/2024es000868

Research Article

Received: 15 February 2023
Accepted: 22 August 2023
Published: 6 May 2024

Introduction

The Zagros Basin has long been considered by researchers due to its significant hydrocarbon reserves and very young tectonic activity, as well as due to the shallowest oil horizon in southwestern Iran. Among these, the sedimentary carbonate platform sediments of the Asmari Formation (Oligo-Lower Miocene) deposited in the Zagros Basin have the greatest development in the Dezful embayment, including some of the largest oil reservoirs in the world and are therefore of particular importance *Bordenave and Hegre* [2005]. The Pyrenean orogenic phase has caused the gradual rise of the mountains of Central and Eastern Iran, Alborz and the formation of the central basins of Iran, the uplift of the Kopedagh and the regression marine of Zagros region. The inland basins of Iran have become playa after the Pyrenean phase. The orogeny phase activity is contemporaneous to the Asmari deposition in the Zagros region.

The type section of Asmari Formation (in Tang Gol Torsh) in Khuzestan province [*Richardson*, 1924] recorded two evaporitic members of Kalhor (southwest of Lorestan and northwest of Dezful embayment) and Ahvaz sandstone (south of Dezful embayment) [*Haidari, Kh. et al.*, 2020; *Yarem Taghloo Sohrabi et al.*, 2019]. The main lithology of Asmari Formation is limestone, dolomite and dolomitic limestone. What is acceptable today about the Asmari Formation was founded by *Lees* [1933]. Asmari base anhydrite, which lies beneath the calcareous layers, is also classified as a part of Asmari. In general, the Formation is continuously deposited on the deeper marine sediments of Pabdeh (Paleocene-Oligocene) and overlain by Gachsaran formations discontinuously in most areas.

The Asmari Formation in the interior Fars region has been studied by various researchers in view of sedimentary environment [*Ahmadi et al.*, 2011; *Akhzari et al.*, 2015; *Mahmoodabadi*, 2014], microfacies [*Dehghanian et al.*, 2012, 2013], facies and biostratigraphy [*Adabi et al.*, 2008; *Allahkarampour Dill et al.*, 2010; *Amirshahkarami et al.*, 2007a,b, 2010; *Bahrami*, 2009; *Ehrenberg et al.*, 2007; *Hakimzadeh and Seyrafian*, 2008; *Karami et al.*, 2020; *Laursen et al.*, 2009; *Nadjafi et al.*, 2004; *Rahmani et al.*, 2009; *Seyrafian and Hamedani*, 2003; *van Buchem et al.*, 2010; *Vaziri-Moghaddam et al.*, 2005], paleoecology and biostratigraphy [*Sooltanian et al.*, 2011], biostratigraphy, paleoecology and diagenesis [*Seyrafian and Hamedani*, 2003].

Therefore, according to the extensive studies of the Asmari Formation in the interior Fars Basin, it seems that there are several geological sections that should be studied. The present study is one of these cases. The main goal of this study is to analysis the microscopic facies, sedimentary environment and the influence of diagenetic processes on the microfacies of Asmari Formation in interior Fars in sections-A, B and C as well as the possible influences of Pyrenean phase activity on the related stratigraphic sequences.

Studied Stratigraphic Sections

To study the sedimentary environment of Asmari Formation in the study area (interior Fars), 3 stratigraphic sections of A, B and C were studied (Figure 1).

Section A is located 140 to 150 km to the SW of Shiraz. Asmari Formation with a thickness of 172.62 meters is located on Pabdeh Formation and below Gachsaran.

Section B is located 86km far from Shiraz in sought-eastern part of the province. The lower boundary of Asmari Formation with Jahrom Formation is discontinuous and its upper boundary with Razak Formation is steep and discontinuous. The thickness of Asmari Formation was 140 m.

Section C is marked on 35 km northwest of Shiraz. The Asmari Formation overlaps Jahrom Formation and its upper boundary is with Gachsaran Formation. The thickness of Asmari Formation in this section is 180 meters (Figure 1).

In view of geological structure, the area understudy is limited by two major faults, Kazerun and Nezamabad which will be described in brief.

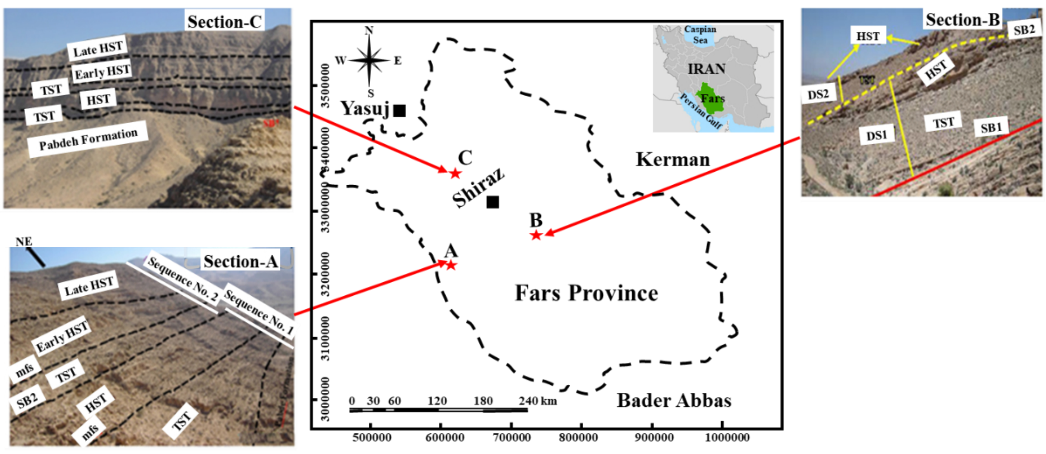

Figure 1. The position map and stratigraphic sections understudy.

Kazerun fault. The Kazerun Fault is known as an active fault zone and defined to be an ancient (Early Cambrian) structural lineament in Zagros region [*Sepehr and Cosgrove*, 2004, 2005, 2007; *Talbot and Alavi*, 1996]. The zone activity controls the characteristics of structure, sedimentation, and subsidence as well as the hydrocarbon system of the belt. The Kazerun Fault has also a major effect on the distribution of the Cambrian Hormuz salt in two areals (more than 100 salt domes in the east and no traces in the west). Its reactivation during the geological time resulted in major sedimentary thickness and facies variations in Zagros and Fars regions.

Nezamabad. Nezamabad fault zone in despite of Kazerun fault is a sinistral strike-slip fault type with the strike of NE-SW. This fault along with Kazerun fault activities have caused complex structural deformations such as variation in axial plane and fold axis or facies changes in the region [*Hosseinpour et al.*, 2019; *Maleki et al.*, 2014, 2015]. However it is claimed that the activity of the Nezamabad fault in this area is limited to Jurassic and Cretaceous periods (Coniacian and Cenomanian) [*Hosseinpour et al.*, 2017], but it is possible to be related to the Kazerun Fault and they have formed a fault system together. The Razak fault is also considered as another structural lineament in the eastern part. All these controlled the geometry of the sedimentary Fars basin as well as later structural deformation.

The final movement of the Iranian-Arabic plates has led to the closure of Neotethys and the creation of a foreland basin. Tectonic activity has played the most important role in the spatial changes of the Zagros Basin, while eustasy has been affected merely in the formation of stratigraphic geometry. It seems that these movements eventually led to the closure of the basin (i.e., after subduction and collision) [*Allahkarampour Dill et al.*, 2010].

Materials and Methodology

In order to study the microscopic facies of Asmari Formation, about 450 thin sections were prepared and studied. The Dunham method [*Dunham*, 1962] has been used to characterize carbonate samples. *Flügel* [2010] and *Wilson* [1975] methods have been used in petrographic study and recognition of mirofacies.

Based on field and petrographic studies of Asmari Formation in all studied sections, a wide range of carbonate facies was identified. To distinguish and identify carbonate facies, factors such as the type of components of carbonate rocks including orthochem, allochem, skeletal and non-skeletal grain types, grain size and their frequency percentage have been used.

Skeletal grains are more common including of miliolid, algae, nummulitid and alveolinid families, as with a higher percentage of milliolide and algae than others. Non-skeletal grains are mostly pellet and intraclast grains, the frequency of which in some samples reaches 50%.

Discussion

Basin analysis is essentially based on sea level changes in local and global scales which is reflected on microfacies frequency in the basin. Therefore, the purpose of this research paper is to compare the effects of Pyrenean orogeny phase in the Asmari Formation in terms of vertical changes of microfacies in different parts of the interior Fars sedimentary basin. In general, according to sequence stratigraphic studies, two sedimentary sequences of third order were identified for Asmari sediments [*Yarem Taghloo Sohrabi et al.*, 2019].

Determined Microfacies

Microscopic examinations of Asmari Formation samples in the studied sections were resulted to identification of 13 carbonate microfacies. According to their vertical change observed in stratigraphic column, these facies were generally deposited in a carbonate shelf type basin during the Oligocene-Miocene period. These facies are classified in the five sedimentary belts including (1) open marine, (2) back reef/barrier, (3) lagoon, (4) shoal and (5) tidal flat (Figure 2).

1. Open marine microfacies

Perforate and imperforate foraminifera packstone (MF1): The facies contains of 85% allochems including the usual hyaline perforate foraminifera of Nummulitids and porcelain imperforate foraminifera including Miliolids and Austrotrilina and a small percentage of intraclast and red algae which are indicating a transitional zone between lagoon and open marine (Figure 3a). Due to the coexistence of red algae and perforate and imperforate foraminifera in the mud, they can be interpreted as a lagoon part adjacent to the platform shoal. Nevertheless, wide spread of hyaline-walled foraminifera can be attributed to the initial parts of the shallow open sea and the middle ramp [*Burchette and Wright*, 1992]. The facies is comparable to RMF-14 and SMF-9.

Perforate foraminifera packstone (MF2): The facies having large benthic foraminfera is hyaline perforate type. Nummulitidae form about 80-90% of the main allochem of this facies (Figure 3b). The facies is indicating a micritic matrix that has been partly glauconitized (Figure 3c). The abundance of perforate foraminifera indicates that these sediments have been deposited in a shallow open sea environment between two key levels (normal waves (fair weather wave base- FWWB) and storm wave base-SWB) [*Beavington-Penney et al.*, 2005]. The environment is characterized by normal salinity and somewhat turbulent. Hematitization process is occurred along stylolites (Figure 4j), dissolved veins, intragrains or vugs (due to weathering) and oxidation of iron bearing minerals as well [*Scholle and Ulmer-Scholle*, 2003; *Tucker et al.*, 2001]. This microfacies is equivalent to RMF-2 and SMF-3.

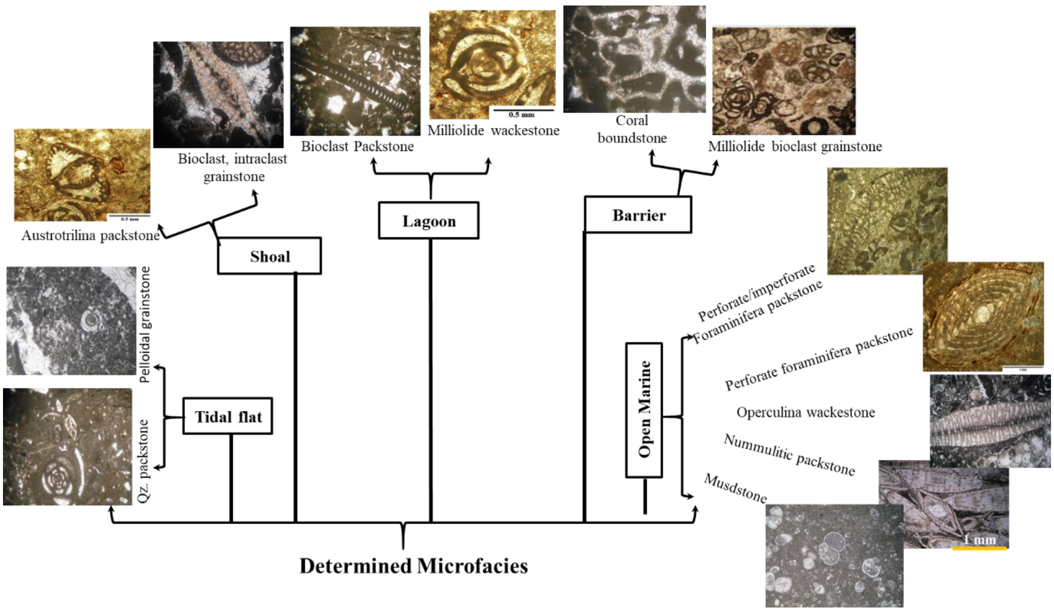

Figure 2. Microfacies and sedimentary belts detected in cross sections understudy of the Asmari Formation.

Operculina wackestone (MF3): The facies is defined by the frequency of hyaline perforate foraminifera, especially Operculina and large and elongated Lepidocyclinides (Nephrolepidina and Eulepidina) in the amount of 40 to 50% and other skeletal (such as echinoderm and bivalve) and non-skeletal (such as pellet) components are less than 10%. Generally, due to the large size of benthic foraminifera, the texture can also be considered as floatstone (Figure 3d). The sedimentary environment is between normal waves and storm surface in a shallow open sea of the middle ramp. The facies is comparable to RMF-2 and SMF-7, 8, 13.

Nummulitidae packstone/wackestone (MF4): It is characterized by the abundance of large perforate benthic such as Nummulitidae and large and elongated Lepidocyclinides with an average frequency of about 20 to 30% and a size of 1.2 to 1.6 mm in the packstone/wackestone matrix. Other skeletal components include coral, red algae, echinoderm, and mollusk (Figure 3e). Sorting and rounding are generally low. The presence of hyaline perforate tests indicates that sedimentation has taken place in the front part of the bar towards the sea [*Vaziri-Moghaddam et al.*, 2010] These are indicating an environment with normal salinity and the lowest sunlight on a carbonate ramp platform. The thinning and widening of these foraminifera occurs with increasing water depth, indicating a decrease in ambient light and energy. The facies is equal to RMF-13 and SMF-2.

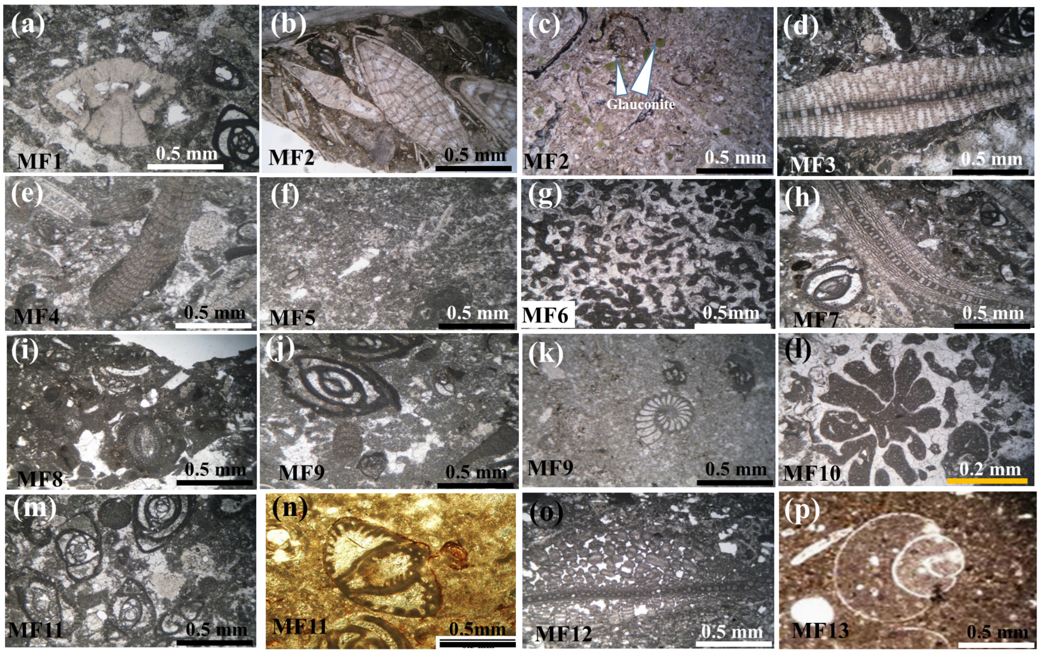

Figure 3. Photomicrographs of selected thin sections of determined microfacies: (a) Perforate and imperforate foraminifera packstone (MF1); (b, c) Perforate foraminifera packstone (MF2); (d) Operculina wackestone (MF3); (e) Nummulitidae packstone/wackestone (MF4); (f) Mudstone (MF5); (g) Coral boundstone (MF6); (h) Miliolidae bioclastic grainstone (MF7); (i) Miliolidae wackestone (MF8); (j, k) Bioclast wackestone/packstone (MF9); (l) Bioclastic (such as Peneropolis sp. and Borelis sp.) grainstone (MF10); (m, n) Austrotrilina packstone (MF11); (o) Peloidal Grainstone (MF12); (p) Quartzeous mudstone/packstone (MF13).

Mudstone (MF5): The facies presents entirely of micritic limestone with less than 10% of planktonic foraminifera (Figure 3f). The presence of deep-sea plankton bioclasts and abundance of micrite indicate a deep sedimentary environment. It is equivalent to RMF-1 and SMF-3.

2. Back reef microfacies

Coral boundstone (MF6): The facies is defined by the presence of in situ coral skeleton, without any fractures or skeletal debris. Granular cement and sometimes calcareous mud have been deposited in inter skeletal grains (inter granular porosity) of corals (Figure 3g). The MF6 was formed in the margin of the platform as patchy reefs which are located above the normal wave level [*Wilson*, 1975]. The porosity types are vuggy, intragranular and fracture. The sedimentary environment is the back reef/barrier and lagoon. The facies is equal to RMF-12 and SMF-7.

Miliolidae bioclastic grainstone (MF7): Skeletal allochems of benthic foraminifera such as Miliolidae and Alveolinidae families are identified with an average abundance of about 60 to 65% in a sparry cement (Figure 3h). This assemblage indicates grains transportation and sedimentation in a barrier island environment [*Ehrenberg et al.*, 2007]. The presence of Miliolidae in grainstone is a marker of very shallow waters, semi/hyper saline state (relatively restricted and high energy) [*Langer and Hottinger*, 2000] MF7 is the most important and abundant microfacies in the Asmari Formation. The cementation process is predominant as sparry calcite which is supported by aragonite dissolution [*Adabi and Rao*, 1991; *Choquette, Ph. W. and James*, 1987; *Tucker and Wright*, 1990]. Furthermore, fenestral porosity is also reported in this condition [*Choquette, Ph. W. and Pray*, 1970] and detected in this area (Figure 4o). The facies is equal to RMF- 8 and SMF-7.

3. Lagoonal microfacies:

Miliolide wackestone (MF8): It is characterized by the frequency of small benthic foraminifera such as Miliolide (0.6 mm) and Ostracod with a less frequency (Figure 3i). The sponge spike is another skeletal component. The size of the components is in the range of lutite (silt to clay size sediments) and sorting is moderate. Bioturbation is the most important sedimentary structure. The sedimentary environment is a restricted lagoon having a relatively high stress conditions [*Flügel*, 2010]. The facies is equal to RMF-20, 26 and SMF-9 and 17.

Bioclastic wackestone/packstone (MF9): It is characterized by a variety of different benthic porcelain imperforate foraminifera including Peneropolis, Dendritina, Miliolidae and Borelis with an average frequency of 40 to 45% in a mud support packstone/wackestone (Figure 3j, 3k). The most important non-skeletal components are peloids and intraclasts with an average frequency of 10 to 15%, which are formed during the micritization process. The sedimentary environment is a lagoon that is confirmed by the lack of normal marine organisms and the abundance of imperforate foraminifera. Comparing to the Miliolidae wackestone, the facies has been deposited in the unrestricted parts of the lagoon due to the higher fossil diversity. This microfacies is equal to SMF-16 and RMF-20.

4. Shoal Microfacies

Bioclastic grainstone (MF10): In this microfacies, the size of foraminifera is high compared to other cases. The amount of lime mud is completely reduced while bioclasts make up the largest amount (55%). In addition to bioclasts such as Bryozoa and Echinoid spines, porcelain crust foraminifera such as Peneropolis and Borelis can be observed with a frequency of 30 to 35%. These bioclastic bars are formed above wave level but lower than the bar height. The intraclast percentage in this facies estimated to 15%. Due to the remove of lime mud, the porosity of the facies increased. All porosity types such as vug (Figure 3l) and fractures can be observed. RMF 26 and SMF-11 and 16.

Austrotrilina packstone (MF11): The facies presents about 40% of the skeletal allochem of the Milliolidae family, and Austrotrilina, which is deposited in a micritic matrix in a shoal environment (Figure 3m, 3n). This is comparable to RMF-26 and SMF-11 and 16.

5. Tidal Flat Microfacies

Peloidal Grainstone (MF12): This belt characterized with individual fauna including of gastropods, red algae and Ostracods. The environment defined by special structures such as lattice or fenestral, gradual graded bedding as well as regular and very thin bedding (Figure 3o). The facies represents a relatively high-energy tidal flat. The facies is equal to RMF-23 and SMF- 21.

Quartzeous mudstone/ packstone (MF13): The facies consists of lime mudstone/ packstone having fine quartz grains (up to 5–15%) in the size of silt to sand (Figure 3p). The frequency of 30% intraclast is significant. Lime to dolomitic mudstones are formed in the interior of tidal mud zones [*Warren*, 2010]. Dolomitization process was developed and dolomite crystals size vary between 16 and 62 microns. The facies is equal to RMF-22 and SMF- 25.

Diagenetic Processes

Thin sections petrographic study indicated that micritization, hematitization, cementation, compaction and pressure solution, dissolution, neomorhism and dolomitiztion are dominant in intervals understudy (Figure 4 and Figure 5).

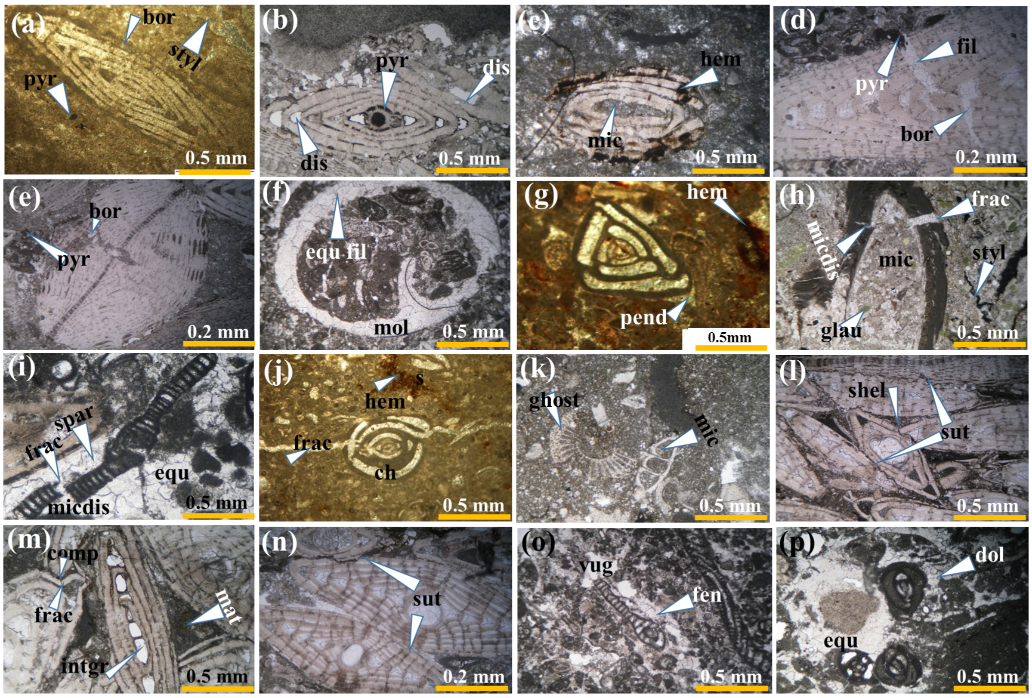

Figure 4. Selected thin sections displaying mirofacies and diagenetic processes in stratigraphic cross sections understudy: (a) Peripheral micritization of the cortex. Micitization is controlled by the location of microborings (arrow), pyritization, stylolitization, (b) pyritization and dissolution, (c) Hematitization and micritization, (d) boring, pyritization and pore filling, (e) boring and pyritization, (f) moldic and equant pore filling, (g) pendant cement beneath a Miliolide, hematitization, (h) Pervasive micritization of allochem, microdisplacement, stylolitization, fracturing, and glauconite, (i) microdisplacement, sparry and equant cement, fracture filling, (j) fracture filling, stylolitization and hematitization, chamber filling, (k) micritization and ghost allochem, (l) compaction and suturing contacts, (m) compaction and fracturing and intragrain porosity, (n) suturing contact and compaction, (o) fenestral and vuggy porosity, (p) sparry and equant cement and dolomite crystals. Abbreviations are: pyr – pyrite; styl – stylolite; dis – dissolution; bor – boring; frac – fracture; intgr – intragrain; mat – matrix; equ – equant; fen – fenestral; sut – suturing; dol – dolomite; he – hematite; shel – shelter; mic – micrite; comp – compaction; ch – chamber; fil – filling; glau – glauconite; mol – moldic; micdis – micro-displacement.

Micritization. *Bathurst* [1966] invented the term micritization to a process of original skeletal grain fabric alteration. The process believed to occur predominantly in shallow marine, or possibly meteoric to shallow burial environments [*Wilson and Evans*, 2002], and marine phreatic environment [*El-Saiy and Jordan*, 2007; *Longman*, 1980]. Micritization is common in the Asmari carbonates (Figure 4e, c, h, k). The data indicated two mechanisms are responsible for the process. The first one involved by micro-borer organisms living at or near the sediment–water interface [*Brigaud et al.*, 2009; *Garcia-Pichel*, 2006; *Llinas*, 2002; *Tucker and Wright*, 1990; *Vincent et al.*, 2007]. Micrite envelopes mostly developed around and within bioclasts as well as in matrix (Figure 4a, i, Figure 5c, j). The second is attributed to thermodynamic variation (alteration process) of environment [*Alexandersson*, 1972; *Carrera*, 2018; *Reid and Macintyre*, 1998; *Salih et al.*, 2019]. In new conditions, the stability of previous large crystals is a function of pressure, temperature and fluids. Therefore, allochem or sparry calcite replaced by micrite which is stable in new conditions. It means that products those are formed as a new fabric and having lower Gibbs energy.

As a main point it should be mentioned that in the studied sections, in most samples (MF-1 to MF-4; MF-8 &9; MF-11 & 13), the micritization process was observed extensively. The process can be occurred during late diagenesis [*Ahmad and Bhat*, 2006; *Sherman et al.*, 1999], or may be due to the microboring activity of endolithic cyanobacteria [*Tucker and Wright*, 1990]. In some cases the micriticization is so severe that only a ghost of allochem remains (Figure 3c, Figure 4h, k).

Hematitization. In some facies of the Asmari Formation cubic pyrite/their hematite pseudomorphs scattered crystals were observed (Figure 4a–d, g, j). These opaque mineral represented reddish color in facies. Their origin is assigned to diagenetic process (telogenetic stage) in the base of DS1 after an erosion period which was dominated by an oxidation environment [*Shogenova and Kleesment*, 2006; *van Houten*, 1973] as well as arid climate [*Shogenova and Kleesment*, 2006]. Therefore, hematite was formed as pore filling (secondary origin) or scattering crystals (authigenic origin) in different diagenetic stages (early or late). Dolomitization process leading to increase of the Fe/Mg ratio and so decreasing the saturation degree of Fe-ion in solution. The process results in to precipitate iron oxides minerals.

Cementation. Cements in the Asmari sediments display a variety of fabrics in different lithofacies comprise of microsparry cement, isopachous cement, granular mosaic cement and pendant cement. Microsparry cement is characterized by microcrystals of relatively equal size (Figure 4i, p, Figure 5d). This cement is observed as pore and fracture filling cement which is most common in marine/meteoric phreatic zones [*Adabi and Rao*, 1991; *Flügel*, 2010], or in burial conditions where meteoric water is more saline [*Flügel*, 2010] as well as in anoxic conditions [*Scholle and Halley*, 1985].

Isopachous cement presents rims growing with equal thickness around allochems (bioclasts or grains) as microcrystalline crystals (Figure 5g–h). This cement is common in marine/vadose environments [*Aghaei et al.*, 2014; *Flügel*, 2010; *Heckel, Ph. H.*, 1983]. Isopachous cements indicate oversaturated fluid environments [*Hosa and Wood*, 2020]. Isopachous fibrous calcite (marine origin) and / or the equant calcite spar (meteoric vadose and phreatic origin) retarded the effect of chemical compaction. Parameters that control the geometry of cemented zones include permeability variations, and the fluids residence time [*Claes et al.*, 2018; *Menke et al.*, 2016, 2017].

Granular mosaic cement is a calcite cement that forms in interparticle pores or in the chambers of bioclasts. The crystals are small (less than 10 µm) and length and width are approximately the same. This cement is the characteristics of the meteoric-vadose and meteoric-phreatic zones as well as burial diagenesis [*Madden et al.*, 2017]. Fractures cutting micritic and clay-rich matrix are filled by a later stage of calcite cement (Figure 4i–j).

Pendant or micro-stalactite-like cement [*Longman*, 1980] forms as droplet beneath the grains within vadose zone. This type of carbonate cement forms in deeper parts of the vadose zone, where more fluid is available, droplets of water can accumulate on the bottoms of grains [*Morse and Mackenzie*, 1990] reflecting the gravity impact (Figure 4g).

Drusy cement forms the lining and pore-filling (intraskeletal chambers) that is common in meteoric and burial environments. The crystal size increases towards the center of pore spaces (Figure 5c, l). This cement is commonly observed in allochem molds such as algae (Figure 5f) and other bioclasts molds.

Compaction (Physical and Chemical Types). The Asmari sediments display compactional effects as physical (mechanical) and chemical features. Physical compaction caused different mechanical mode such as slippage, deformation contact and fracturing and also decrease of primary interparticle porosity in grain-supported facies (Figure 4i, l, m–o). Skeletal (e.g., foraminifera, and echinoderms) and non-skeletal grains (pellet and clast) have been fractured. In view of burial chemical compaction some of the sediment characteristics were changed. The main feature is pressure solution and stylolitization (Figure 4a, h).

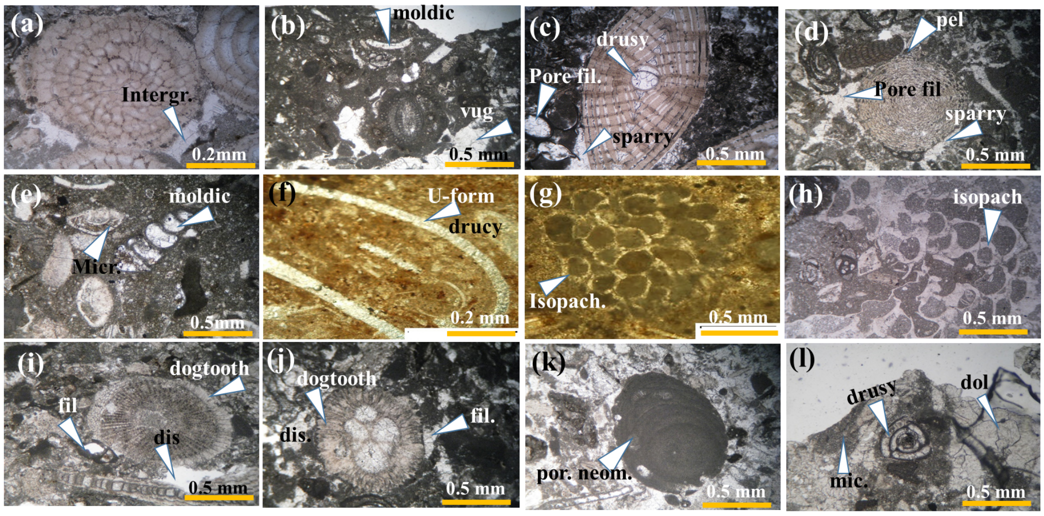

Figure 5. Selected thin sections indicating diagentic processes in area under study: (a) Intergrains porosity, (b) vuggy and moldic porosity, (c) drusy and sparry cements, pore filling, (d) peloidal and sparry cements and pore filling, (e) moldic porosity and micritization, (f) algae moldic and drusy cement, (g, h) isopachous cement, (i, j) dissolution, peripheral dogtooth cement and pore filling, (k) porphyroid neomorphism, (l) micritization, dolomitization and drusy cement. Abbreviations are: mic – micrite; dol – dolomite; por – pore; fil – filling; dis – dissolution; isopach – isopachous; intergr – intergranular; pel – pellet.

Dissolution. The process is extensively occurred as partial dissolution (Figure 5a–f) or oversize pores. Moldic dissolution in the studied samples was pervasive. The moldic pores are filled with blocky cements, indicating a very early process [e.g., *Arzaghi and Afghah*, 2014; *Brigaud et al.*, 2009]. Secondary porosity was generated by dissolution of grains and may be filled by blocky calcite. In some cases peloidal cement is also observed (Figure 5d).

Neomorphism/Recrystallization. Neomorphism is occurred in two types: dissolution and recrystallization [e.g., *Lakshtanov et al.*, 2018] and solid state crystallization [*Bathurst*, 1972; *Dickson*, 1978]. In the first mechanism, recrystallization requires dissolution in pore fluids and precipitation on existing pores. The process is dominant in burial diagenesis. The presence of organic compounds has an important influence on recrystallization kinetics and acts as an inhibitor factor [*Lakshtanov et al.*, 2018]. The second process which is common during diagenesis is solid state recrystallization. Recrystallization refers to any change (crystal volume, crystal shape or crystal lattice orientiation) in the fabric of a mineral or monomineralic sediment [*Bathurst*, 1972]. The most visible characteristic of limestone in diagenesis is the increase of calcite crystal size (sparry content). The neomorphism process is pervasive and observed in most samples understudy as pore filling (Figure 5a–f, j-l) and porphyroid states (Figure 5k). Peripheral dogtooth replacement (cement) was also formed (Figure 5i, j).

Dolomitization. Dolomitization is not pervasive in the Asmari sections except in individual horizons (MF-9 and MF-13). Based on dolomite fabric study [e.g., *Sibley and Gregg*, 1987], dolomites are fine to medium euhedral crystals (16–62 µm) and the size is up to 60 µm These crystals are separated by mud (Figure 4p, Figure 5l) which are the residue of initial matrix. The euhedral dolomite rhombs mostly having cloudy or dusty cores resemble possible chemical variation from Fe rich in the inner core to Mg rich in outer parts of cores.

This is documented using Alizarine red-S to differentiate calcite and non-ferroan dolomite [*Coniglio et al.*, 2004]. Clear dolomite cements forms the edges of the rhombs.

Porosity. Porosity type depends on the facies and should be fabric control, and in some cases also related to deformation stresses. As evident from microscopic study, grains contain microfractures that those are straight-curvature traces, and in some cases formed veins (Figure 4h, i, j). These veins have been filled by sparry calcite. Compaction and tectonic stresses are responsible to produce these fractures [*Poursoltani and Harati-Sabzvar*, 2019]. Vuggy (Figure 5a), moldic (Figure 5b, e–f, l), dissolution (Figure 5i–j), intergrain (Figure 5a) and intragrain (Figure 5b, e), fenestral (Figure 5o) porosity types as well as fracture type (e.g., Figure 4h) can be observed in samples studied.

Depositional Sequence (DS) of the Studied Sections

Sedimentary sequence boundaries are the result of subaerial discontinuities [*Vail and Mitchum*, 1977; *Vail et al.*, 1977a,b,c] The discontinuity is spatially equal to the sea water fall stage at the lowest level on the shoreline [*Catuneanu*, 2002]. Correlation concordance (sediment surface is equal to the terrestrial discontinuity surface) can be adapted to the sea floor at the beginning of a regression phase [*Haq et al.*, 1987, 1988; *Posamentier and Jervey*, 1988; *Posamentier and Vail*, 1988]. Nevertheless, there is another interpretation invoked by other researchers that this level is compatible with the sea floor at the end of the regression phase [*Christie-Blick*, 1991; *van Wagoner et al.*, 1988, 1990, 1991]. Although this idea agreed upon by some, *Hunt and Tucker* [1992, 1995], Hunt and Tucker, 1992, 1995, as well as *Plint* [1990] and *Plint and Nummedal* [2000], introduced a term of Falling stage systems tract (FSST), which is equal to a regression phase. Correlation is however difficult to detect in the shallow sea and can be detected through seismic data, but in the deep sea, it is easy to detect the submarine cone system below the sea level fall [*Catuneanu*, 2002; *Catuneanu et al.*, 2009a,b].

Two types of depositional sequences (DS) were identified through sedimentary facies analysis in this area including DS1 and DS2 (Figure 6). Sequence boundaries (SB) are determined by facies changes. In this regards, SB as either type 1 or type 2 are considered as a function of the rate of global sea-level fall or local sediment accommodation and [*Catuneanu et al.*, 2011; *McLaughlin*, 2005; *Patzkowsky and Holland*, 2012; *van Wagoner et al.*, 1988]. It can be also inferred that the subsidence rate is different in two types. Type 1 sequence boundary reflects an intense subaerial erosion comparing to type 2 which is characterized by a change in facies-stacking patterns as well as is minor in view of the basinwards shift in facies. So type 2 sequence boundary exhibits in contrast to type 1 sequence boundary, only little subaerial exposure [*van Wagoner et al.*, 1988].

First Depositional Sequence (DS1). In the section A (Rupelian to Chattian) in Oligocene, this sequence is limited by the Pabdeh Formation in the lower part as SB2 type and Gachsaran Formation in the upper part as SB2 type (falling sea level with a slow rate) (Figure 6 section A). The Asmari Formation with 102 m thick consisting of a sedimentary sequence of two strata of Transgressive Systems Tract (TST) (presents offshore environment sediments with the thickness of 40 m), and Highstand Systems Tract (HST) (the sediments of back reef/barrier and lagoon environments forming a thickness of 62 m) deposits. In view of overlapping parasequences the pattern of TST facies is a regressive one, and in HST is a fixed or growth form. The frequency of foraminifera are marked by agglutinated, hyaline and macrospheric shells in TST and microspheric forms in HST.

In section B (Rupelian-lower Aquitanian), this sequence with the thickness of 70 m presents SB1 type with Jahrom Formation and SB2 type boundary in Asmari Formation (Figure 5, section B). The thickness of TST facies (is about 20 m of sediments that are deposited in open sea condition. HST sediments with the thickness of 50 m are composed of bar and back barrier facies with the increasing layer thickness upward.

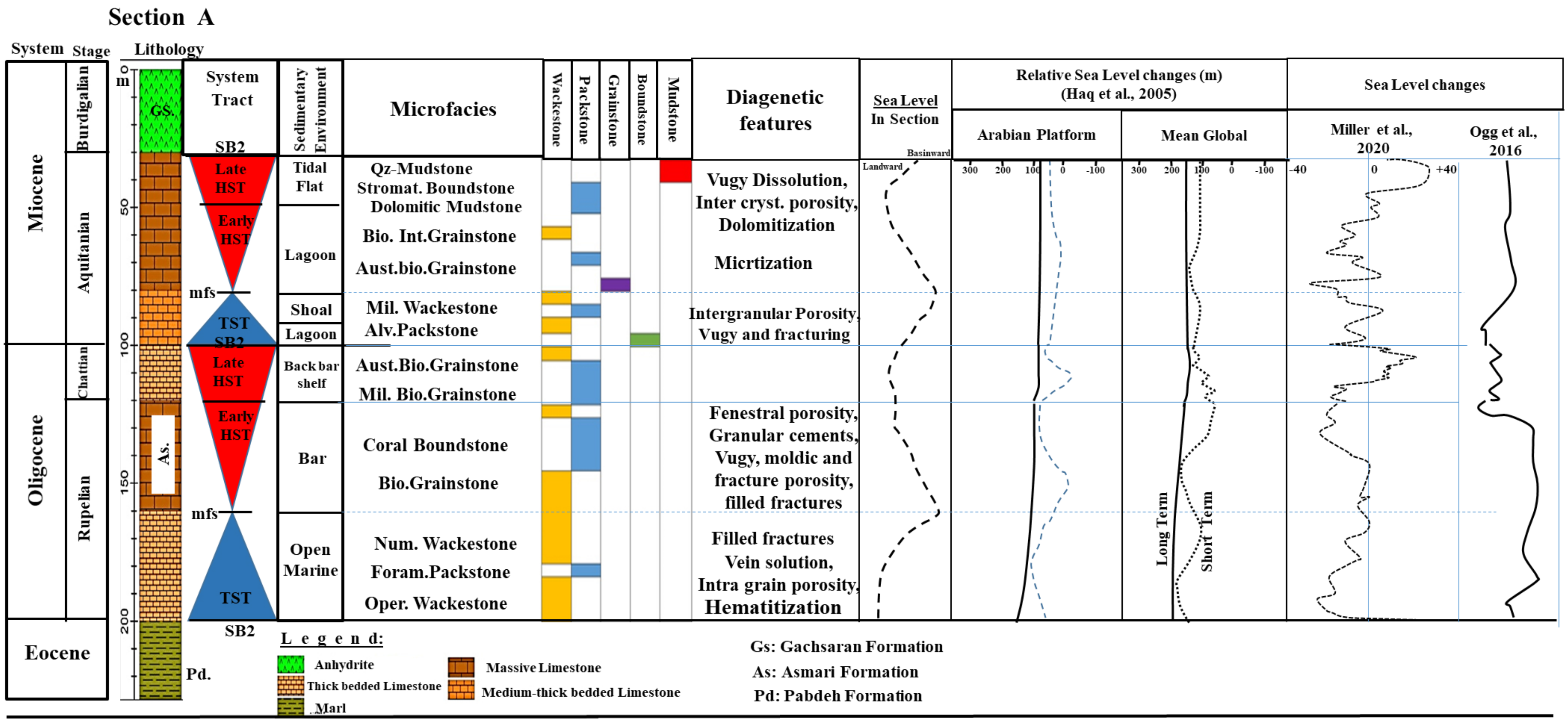
Section A
System
Stage
Lithology
Miocene
Oligocene
Eocene
Burdigalian
Aquitanian
Chattian
Rupelian
GS.
As.
Pd.
System Tract
SB2
Late HST
Early HST
mfs
TST
Sedimentary Environment
Tidal Flat
Lagoon
Shoal
Back bar shelf
Bar
Open Marine
Microfacies
Qz-Mudstone
Stromat. Boundstone
Dolomitic Mudstone
Bio. Int.Grainstone
Aust.bio.Grainstone
Mil. Wackestone
Alv.Packstone
Aust.Bio.Grainstone
Mil. Bio.Grainstone
Coral Boundstone
Bio.Grainstone
Num. Wackestone
Foram.Packstone
Oper. Wackestone
Wackestone
Packstone
Grainstone
Boundstone
Mudstone
Diagenetic features
Vugy Dissolution,
Inter cryst. porosity,
Dolomitization
Micrtization
Intergranular Porosity,
Vugy and fracturing
Fenestral porosity,
Granular cements,
Vugy, moldic and fracture porosity,
filled fractures
Filled fractures
Vein solution,
Intra grain porosity,
Hematitization
Sea Level In Section
Landward
Basinward
Relative Sea Level changes (m) (Haq et al., 2005)
Arabian Platform
Mean Global
Long Term
Short Term
Sea Level changes
Miller et al., 2020
Ogg et al., 2016
Legend:
Anhydrite
Thick bedded Limestone
Marl
Massive Limestone
Medium-thick bedded Limestone
Gs: Gachsaran Formation
As: Asmari Formation
Pd: Pabdeh Formation

(a)

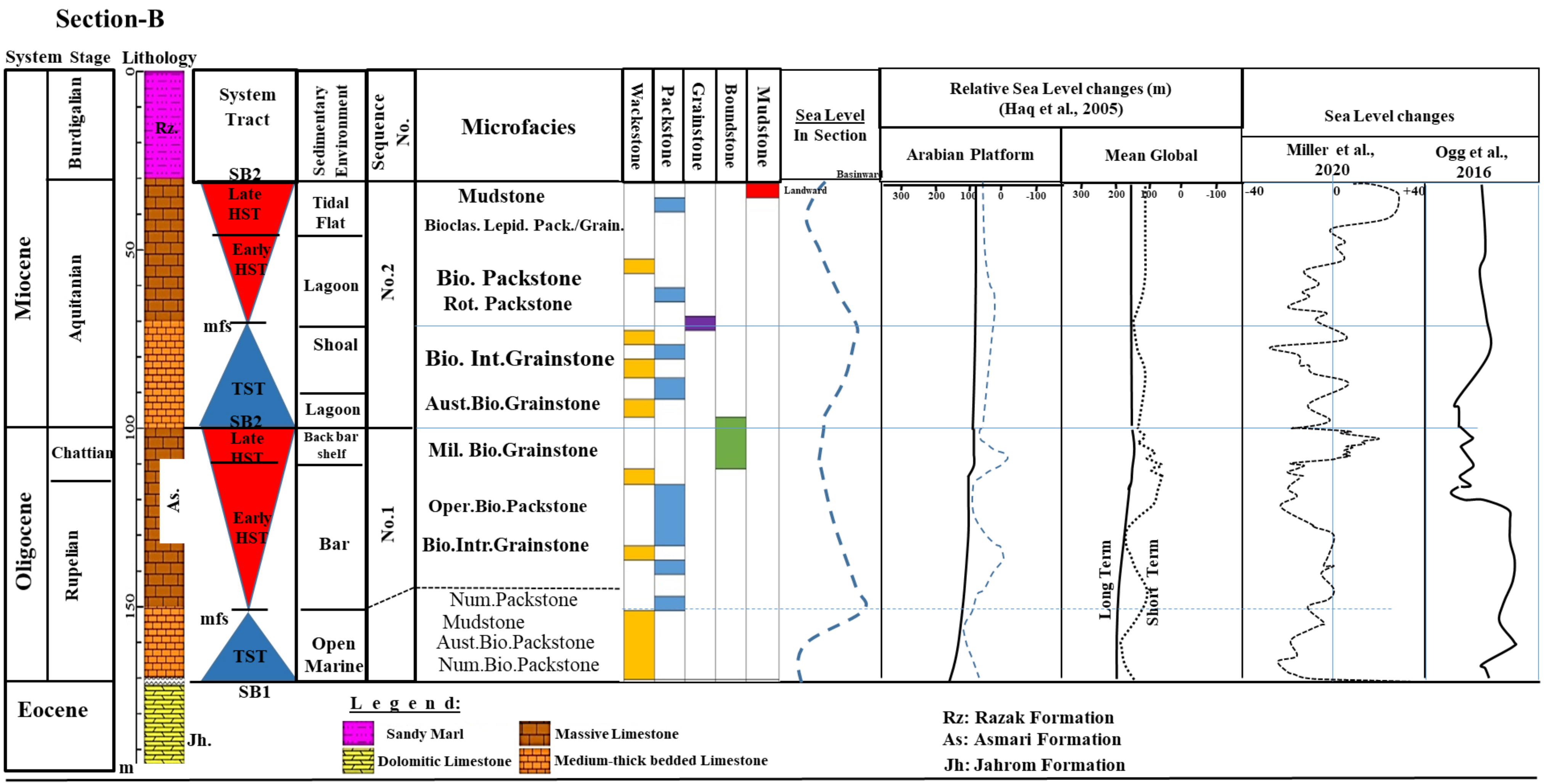
Section-B
System
Stage
Lithology
Miocene
Burdigalian
Aquitanian
Oligocene
Chattian
Rupelian
Eocene
Rz.
As.
Jh.
System Tract
SB2
Late HST
Early HST
mfs
TST
SB1
Sedimentary Environment
Tidal Flat
Lagoon
Shoal
Back bar shelf
Bar
Open Marine
Sequence No.
No.2
No.1
Microfacies
Mudstone
Bioclas. Lepid. Pack./Grain.
Bio. Packstone
Rot. Packstone
Bio. Int.Grainstone
Aust.Bio.Grainstone
Mil. Bio.Grainstone
Oper.Bio.Packstone
Bio.Intr.Grainstone
Num.Packstone
Aust.Bio.Packstone
Num.Bio.Packstone
Wackestone
Packstone
Grainstone
Boundstone
Sea Level In Section
Landward
Basinward
Relative Sea Level changes (m) (Haq et al., 2005)
Arabian Platform
Mean Global
Long Term
Short Term
Sea Level changes
Miller et al., 2020
Ogg et al., 2016
Legend:
Sandy Marl
Dolomitic Limestone
Massive Limestone
Medium-thick bedded Limestone
Rz: Razak Formation
As: Asmari Formation
Jh: Jahrom Formation

(b)

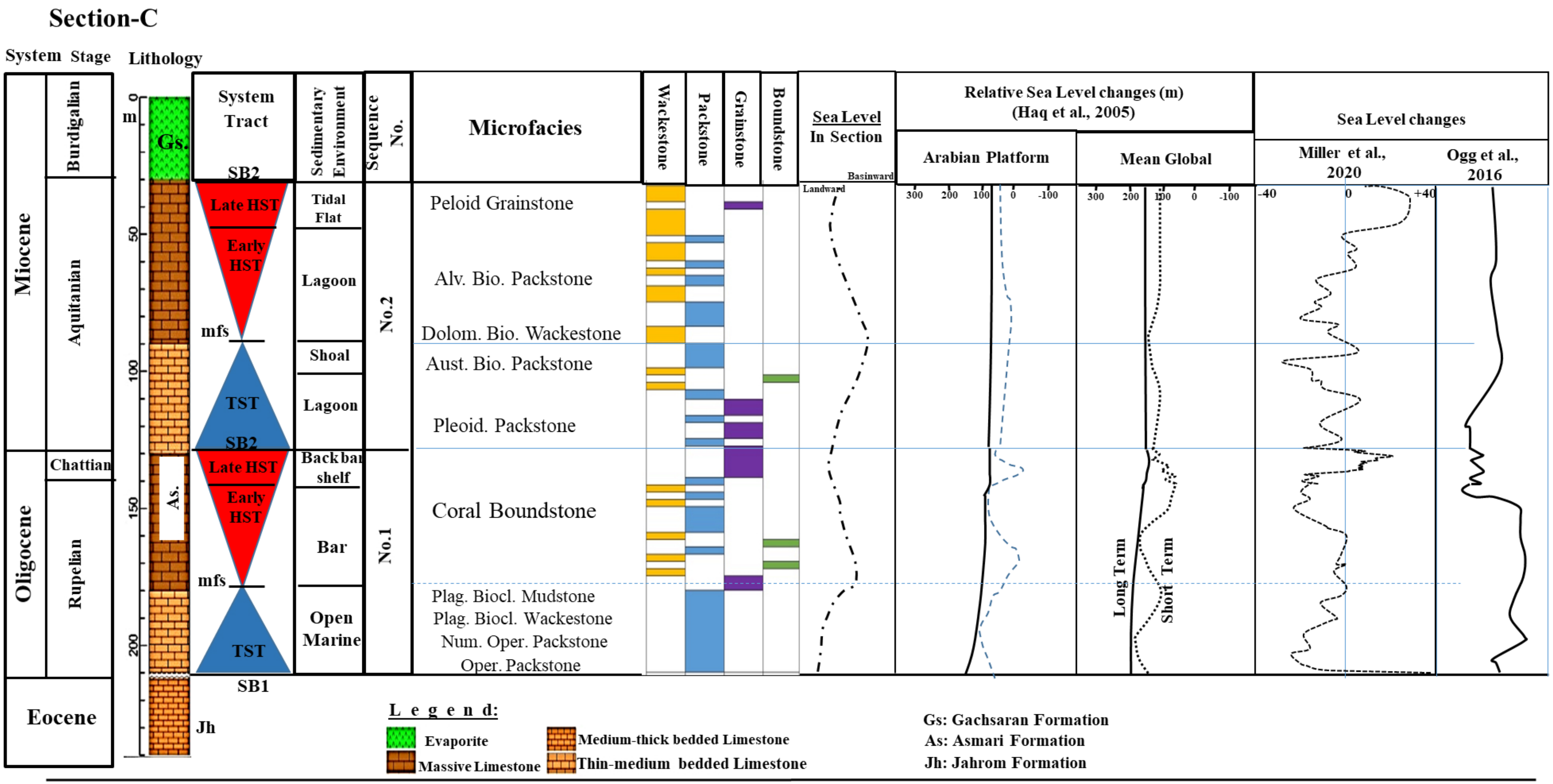

(c)

Figure 6. Lithostratigraphic facies and stratigraphic columns correlation of the Asmari Formation in different sections under study along with the sea level changes in the section comparing to the patterns of global sea level changes [*Ogg et al.*, 2016] and Arabian plate [*Haq and Al-Qahtani*, 2005].

In section C (Rupelian to Chattian) with a thickness of about 80 meters which are deposited in two parts that 30 m in TST (open sea facies) and 50 m during HST period (barrier and the back barrier facies) (Figure 6, section C). These sediments show an increase in the layer thickness. The lower boundary of the sequence with the Pabdeh Formation is erosive (SB1 type) while the upper boundary is (SB2 type).

Second Depositional Sequence (DS2). The thickness of this sequence (Aquitanian) in the section A is 70 m, the lower and upper border is of SB2 type. The sequence presents thin layers. The thickness of TST facies (lagoon) is 21 m and HST facies (shoal and tidal flat) is 49 m. In view of the type of parasequence pattern, TST and HST facies show a regressive trend. The abundance of porcelain foraminifera in the HST facies is a main characteristic (Figure 6, section A).

Section B: This sequence with a thickness of 70 m consists of TST facies with a thickness of 30 m of middle to thick limestone layers with the sequence boundary of SB2 type deposited in lagoon and shoal environments. The TST sediments is followed by the HST facies with a thickness of 40 m of sediments deposited in lagoon and tidal flat environments. The HST sediments are limited by Jahrom Formation and Razak Formation (SB2) (Figure 6, section B).

Section C: This sequence (Aquitanian-Burdigalian) with a thickness of 100 m composed of TST facies (40 m) including thin to medium layer of limestone with the SB2 and HST facies (60 m) which are deposited in lagoon and shoal environment. The lower boundary of the sequence (with Pabdeh Formation) is SB1 and upper boundary (with Gachsaran Formation) is SB2 (Figure 5, section C). In general, the erosive discontinuity in the lower boundary of Asmari Formation in sections B and C can be ascribed to the Pyrenean phase activity in this region.

Sea Level Changes in the Area Understudy

The basin evolution in the area understudy is a geological part which is influenced by the Arabian platform events. The Arabian plate is undergoing a complex transformation history that has been strongly influenced by global sea level change. Although the Arabian shield remained relatively constant during the Phanerozoic period, the stratigraphy of the Arabian platform and pre-existing basin before the platform origin show a record of second- and third-cycle sequences differentiated by extensive local discontinuities. These erosive hiatus, or sediment-free hiatus, are created by large tectonic events on the margins of the platforms. An indication of these tectonic events is a change in the subsidence rate that has created or destroyed the sediment accumulation surfaces. Therefore, both eustasy and tectonic play a major role in the development of sedimentary sequences, the identification of the characteristics of reservoir and caprock facies on the Arabian plate [*Haq and Al-Qahtani*, 2005].

In the Late Eocene, the Arabian plate, after colliding with Asia, caused the closure of Neotethys Ocean and ended near the Late Oligocene. The movement of the Arabian plate to the northeast led to rifting of the western margin and exerted pressure to the northeast. The rifting process of the Gulf of Aden and the Red Sea may have begun in the Late Oligocene [*Hughes and Beydoun*, 1992; *Hughes and Filatoff*, 1995; *Hughes and Johnson*, 2005; *Hughes et al.*, 1991, 1992, 1999] but was fully apparent in the Middle Miocene-Late Miocene. It is likely that the pressure exerted by the eastern part has supported the bending of the plate [*Sharland et al.*, 2001].

The basins of Iran and Turkey have been subjected to a number of tectonic events that are partially responsible for reactiviation local tectonic structures and the diversity of platform deposits. Platform maximum flooding surfaces (MFS) or transgression of the shelf are first detected by TST sediments that is covered by HST sediments. LST sediments equivalents are maintained only on the platform within the valleys (as residual sediments). Although *Sharland et al.* [2001] did not recognize sequence boundaries, but they did attempt to classify the main MFS events and connect them locally. Detection of main local MFS events is very useful for drawing onlap curves. The effects of major tectonic events are divided into two categories: local (Arabic plate) and global responses [*Geert et al.*, 2001; *Grabowski and Norton*, 1995; *Haq and Eysinga*, 1998; *Sharland et al.*, 2001].

Long-term paleo-climate and paleo-oceanographic events are among the events that have taken place in surrounding of the Arabian platform, just like global events. Most of these events, based on the theories of *Sharland et al.* [2001], have been applied to local glaciers or to other global events [*Haq and Eysinga*, 1998]. The earliest period of the original hiatus (over 10 m.y.) occurred in the Oligocene, which may be a sign that the Arabian plate collided with Eurasia plate and the easternmost part of the Neotethys Ocean closed. A sea level fall also began during the Late Eocene, due to the expansion of the main ice cap ridges at the poles [*Haq and Al-Qahtani*, 2005].

The fault movement during the Middle Cretaceous using the isopach and facies maps of the Zagros indicates that the Kazerun fault zones and other basement faults (N-S trending structures) has also been generated several paleohighs [*Koop and Stoneley*, 1982; *Setudehnia*, 1978]. Salt diapirs upwelling along the fault zone is also another factor which are controlled the structural deformation style [e.g., *Player*, 1969]. All evidences indicated that there is no oil potential in the Fars region. It seems that the combination of all these parameters involved to introduce different subsidence rates in the basin. However, in the Late Cretaceous and early Tertiary the onset of collision was added as another important factor to support more heterogeneity in sedimentary sequences.

The role of pre-existing structures such as Kazerun, Nezamabad and Razak faults is important during the building of the Zagros-Fars basins. Reactivation of these inherited pre-existing faults occurred at the Cretaceous time [*Razavi Pash et al.*, 2021]. Therefore, sea level changes pattern in different geological section understudy revealed that those trends are relatively similar to that of Arabian plate during the time span of the Asmari deposition. These patterns are also comparable with the global sea level changes. However, there is some dissimilarity (such as sedimentary facies changes, the formation below the lower boundary of the Asmari Formation, the lack of coral deposits during the Rupelian of the section B) due to the local variation affected by internal factors.

Sedimentary Facies Changes and Pyrenean Orogeny Phase Relation

Microfacies analysis in the studied stratigraphic sections shows two sedimentary sequences of third order with differences in the thickness of stratigraphic sections. In sections B and C, it is affected by regional tectonics and starts with erosion discontinuity. Also, in section C, the essential conditions have been developed for the formation of coral facies. This stratigraphic correlation reveals that factors other than eustasy process have controlled the distribution of Asmari facies. However, the small-scale changes of global sea level variation on the Asmari Formation are highly influenced locally.

The changes in the relative curves of the sea level for the studied sections are in good agreement with the sequences of the Arabic plate pattern. In these stratigraphic sections, the upper and lower contact surfaces of the Asmari sequence correspond to the decrease in sea level on a global scale; the observed differences are probably due to internal tectonic processes (Figure 7). In this regard, reactivation of faults such as Kazerun and Nezamabad faults along with changes in sea level and the effects of Alpine orogenic phases (i.e., Pyrenean phase) have played a major role in changes in stratigraphic thickness and geometry of the basin (Figure 8).

These faults reactivation seems to be the main controlling factors of the basement deformation [*Razavi Pash et al.*, 2021]. It seems this feature has been affected on the sedimentation rate and microfacies distribution in the interior Fars Basin during Asmari deposition. As well as they impacted on the hydrocarbon potential of this area [*Hosseinpour et al.*, 2017]. These activities are most probably more intense in the northern section (section C) than other parts in the area understudy respect to observed sequence boundary type and sediments thickness.

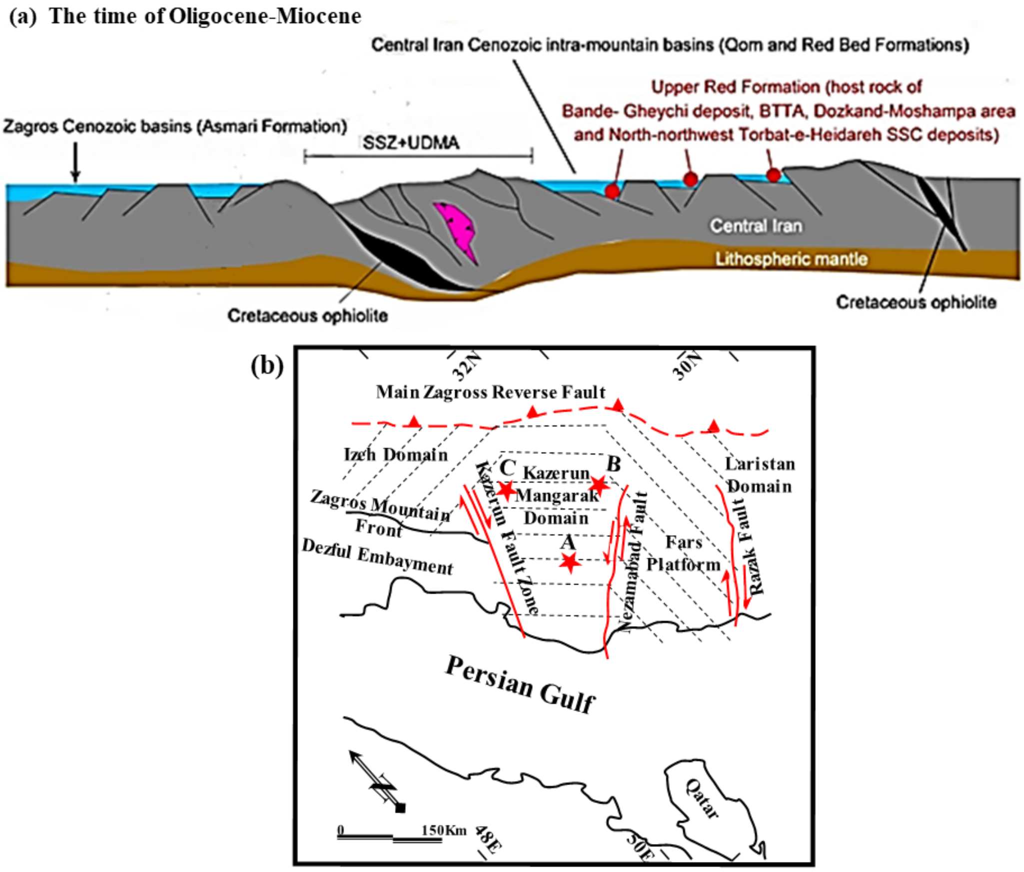

Figure 7. (a) Structural cross sections of the Asmari Formtion during Oligo-Miocene period [*Maghfouri et al.*, 2020] and (b) faults positions which are bounded the Fars platform [*Razavi Pash et al.*, 2021].
*Notes: UDMA – Urumieh-Dokhtar Magmatic Arc, SSZ – Sanandaj-Sirjan Zone.

Therefore it seems that several factors such as local and global sea level scales, and fault activity (due to Alpine orogeny in particular or with emphasis to Pyrenean phase) during the Asmari deposition influenced on sedimentary facies distribution. Thus, it is impossible to ignore them in the interpretation of microfacies development, sedimentary sequences, and basin analysis.

Conclusion

Microfacies distribution and sea level changes in 3 studied stratigraphic sections of Asmari Formation provided the following main points concerning to the sedimentary basin analysis in the interior Fars region (south of Iran).

There is a specific discontinuity between Asmari Formation and Jahrom Formation (in lower part) in section B which is not observed in the other stratigraphic sections.

Microscopic thin sections study of the Asmari Formation samples led to identify 13 microfacies that were deposited in 5 belts on a carbonate platform (carbonate shelf type) during the time span of Oligocene-Miocene. Sedimentary environment and microfacies variation from the basin towards the shallow conditions are of (a) Open sea (including of MF1 – packstone with perforate and imperforate foram, MF2 – packstone with perforate foram, MF3 – Operculina wackestone, MF4 – Nummulitidae wackestone/packstone, and MF5 – Mudstone), (b) bar (MF6 – coral boundstone, MF7 – Miliolide bioclastic grainstone), (c) Lagoon (MF8 – Miliolide wackestone, MF9 – bioclast wackestone/packstone), (d) shoal (MF10 – intraclast bioclast grainstone, MF11 – Austrotrilina grainstone), (e) tidal flat (MF12 – pelloidal grainstone, MF13 – Quartz bearing packstone/mudstone).

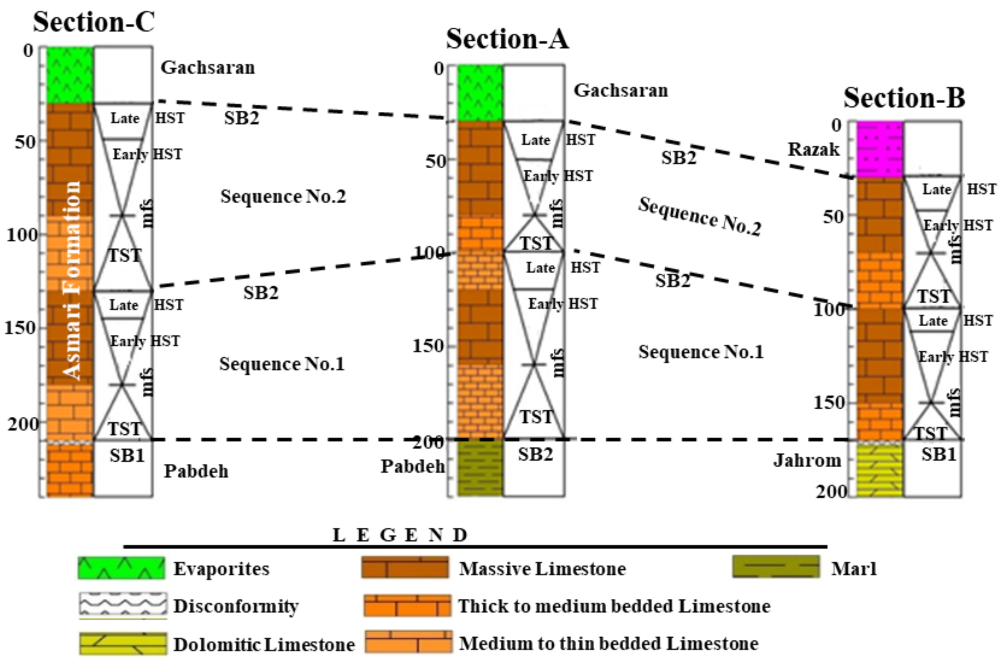

Figure 8. Sedimentary sequences correlation in different cross sections understudy.

*Notes: HST – Highstand System Tract, LST – Lowstand System Tract, SB – Sequence Boundary, MFS – Maximum Flooding Surface.

The Asmari sediments was affected intensely by diagenetic processes such as micritization, hematitization, cementation, compaction and pressure solution, dissolution, neomorhism and dolomitization. These processes are dominant in 3 geological sections understudy. Porosity is also varied and controlled by sedimentary fabric. The porosity types are including of vuggy, moldic, dissolution, intergrain, intragrain, and fenestral as well as fracture type. The presence of fractures along with fine dislocations is evidence of active tension in the area.

Microfacies variation and global sea level changes of sequence stratigraphic understudy not only appeared two sequences of third order but also revealed the effect of Pyrenean phase activity in this area as well as reactivation of faults. This activity is supported by the presence of the erosion discontinuity in the lower boundary of Asmari Formation with Jahrom and Pabdeh formations in geological cross sections of B and C.

The present results evidenced that several factors such as local and global sea level changes, and fault activity (Pyrenean phase) during the Asmari deposition are influenced on sedimentary facies distribution. Thus, fault activity analysis is so important in this province to get the accurate facies interpretation and structural deformation. Therefore, it is proposed to involve their effects in the Fars basin analysis and petroleum aspects interpretation.

Acknowledgments. I thank the K-NET and KiK-net Digital Strong-Motion Seismograph Network of Japan for the records of the 2024 Noto earthquake and the profiling data. The work was supported by RSF grant 23-27-00316.

References

Adabi, M. H., and C. P. Rao (1991), Petrographic and geochemical evidence for original aragonite mineralogy of upper Jurassic carbonates (Mozduran formation), Sarakhs area, Iran, *Sedimentary Geology*, *72*(3–4), 253–267, https://doi.org/10.1016/0037-0738(91)90014-5.

Adabi, M. H., A. Zohdi, A. Ghabeishavi, and H. Amiri-Bakhtiyar (2008), Applications of nummulitids and other larger benthic foraminifera in depositional environment and sequence stratigraphy: an example from the Eocene deposits in

Zagros Basin, SW Iran, *Facies*, *54*(4), 499–512, https://doi.org/10.1007/s10347-008-0151-7.

Aghaei, A., A. Mahboubi, R. M. Harami, M. Nadjafi, and G. J. Chakrapani (2014), Carbonate diagenesis of the upper Jurassic successions in the west of Binalud - Eastern Alborz (NE Iran), *Journal of the Geological Society of India*, *83*(3), 311–328, https://doi.org/10.1007/s12594-014-0044-z.

Ahmad, A. H. M., and G. M. Bhat (2006), Petrofacies, provenance and diagenesis of the dhosa sandstone member (Chari Formation) at Ler, Kachchh sub-basin, Western India, *Journal of Asian Earth Sciences*, *27*(6), 857–872, https://doi.org/10.1016/j.jseaes.2005.08.005.

Ahmadi, V., A. Zavarei, A. Motaharian, and M. Munt (2011), Gastropods identification of Asmari Formation in Shamsabad and Runiz stratigraphic sections in south-east of Shiraz (Fars Province), *Scientific Quaternary Journal of Geosciences*, *21*(8), 95–102, https://doi.org/10.22071/GSJ.2011.54445.

Akhzari, S., A. Seyrafian, and H. Vaziri-Moghaddam (2015), Oligocene microfacies and sedimentary environment of the Asmari Formation at northwest of Deris village, west of Fars province and thickness, age and sedimentary environment correlation with three other sections in Zagros Basin, *Iranian Journal of Petroleum Geology*, *5*(9), 43–58 (in Persian).

Alexandersson, T. (1972), Micritization of carbonate particles: processes of precipitation and dissolution in modern shallow-marine sediments, *Bulletin of the Geological Institution of the University of Upsala*, *3*(7), 201–236.

Allahkarampour Dill, M., A. Seyrafian, and H. Vaziri-Moghaddam (2010), The Asmari Formation, north of the Gachsaran (Dill anticline), southwest Iran: facies analysis, depositional environments and sequence stratigraphy, *Carbonates and Evaporites*, *25*(2), 145–160, https://doi.org/10.1007/s13146-010-0021-6.

Amirshahkarami, M., H. Vaziri-Moghaddam, and A. Taheri (2007a), Sedimentary facies and sequence stratigraphy of the Asmari Formation at Chaman-Bolbol, Zagros Basin, Iran, *Journal of Asian Earth Sciences*, *29*(5–6), 947–959, https://doi.org/10.1016/j.jseaes.2006.06.008.

Amirshahkarami, M., H. Vaziri-Moghaddam, and A. Taheri (2007b), Paleoenvironmental model and sequence stratigraphy of the Asmari Formation in Southwest Iran, *Historical Biology*, *19*(2), 173–183.

Amirshahkarami, M., A. Ghabishavi, and A. Rahmani (2010), Biostratigraphy and paleoenvironment of the larger benthic foraminifera in wells sections of the Asmari Formation from the Rag-e-Safid Oil Field, Zagros Basin, Southwest Iran, *Stratigraphy and Sedimentology Researches*, *26*, 63–84.

Arzaghi, S., and M. Afghah (2014), Diagenetic aspects of the Lower Paleocene Sachun Formation carbonates, Zagros Basin, southwestern Iran, *Journal of Earth Science*, *25*(5), 884–894, https://doi.org/10.1007/s12583-014-0480-0.

Bahrami, M. (2009), Stratigraphy, microfacies and sedimentary environments of Asmari Formation at Tang-e-Bolhayat, north of Kazerun, Fars Province, Iran, *Geophysical Research Abstracts*, *11*(EGU2009-4728).

Bathurst, R. G. C. (1966), Boring algae, micrite envelopes and lithification of molluscan biosparites, *Geological Journal*, *5*(1), 15–32, https://doi.org/10.1002/gj.3350050104.

Bathurst, R. G. C. (1972), Neomorphic Processes in Diagenesis, in *Carbonate Sediments and their Diagenesis*, chap. 12, pp. 475–516, Elsevier, https://doi.org/10.1016/s0070-4571(08)70906-3.

Beavington-Penney, S. J., V. Paul Wright, and A. Racey (2005), Sediment production and dispersal on foraminifera-dominated early Tertiary ramps: the Eocene El Garia Formation, Tunisia, *Sedimentology*, *52*(3), 537–569, https://doi.org/10.1111/j.1365-3091.2005.00709.x.

Bordenave, M. L., and J. A. Hegre (2005), The influence of tectonics on the entrapment of oil in the dezful embayment, Zagros foldbelt, Iran, *Journal of Petroleum Geology*, *28*(4), 339–368, https://doi.org/10.1111/j.1747-5457.2005.tb00087.x.

Brigaud, B., Ch. Durlet, J.-F. Deconinck, B. Vincent, J. Thierry, and A. Trouiller (2009), The origin and timing of multiphase cementation in carbonates: Impact of regional scale geodynamic events on the Middle Jurassic Limestones diagenesis (Paris Basin, France), *Sedimentary Geology*, *222*(3–4), 161–180, https://doi.org/10.1016/j.sedgeo.2009.09.002.

Burchette, T. P., and V. P. Wright (1992), Carbonate ramp depositional systems, *Sedimentary Geology*, *79*(1–4), 3–57, https://doi.org/10.1016/0037-0738(92)90003-A.

Carrera, M. F. L. (2018), Diagenesis characterization and modeling of carbonate rocks: application to Mississippian lime (Oklahoma, United States of America), phdthesis.

Catuneanu, O. (2002), Sequence stratigraphy of clastic systems: concepts, merits, and pitfalls, *Journal of African Earth Sciences*, *35*(1), 1–43, https://doi.org/10.1016/S0899-5362(02)00004-0.

Catuneanu, O., V. Abreu, J. P. Bhattacharya, M. D. Blum, R. W. Dalrymple, et al. (2009a), Towards the standardization of sequence stratigraphy, *Earth-Science Reviews*, *92*(1–2), 1–33, https://doi.org/10.1016/j.earscirev.2008.10.003.

Catuneanu, O., V. Abreu, J. P. Bhattacharya, M. D. Blum, R. W. Dalrymple, et al. (2009b), Reply to the comments of W. Helland-Hansen on "Towards the standardization of sequence stratigraphy" by Catuneanu et al. [Earth-Sciences Review 92(2009)1-33], *Earth-Science Reviews*, *94*(1–4), 98–100, https://doi.org/10.1016/j.earscirev.2009.02.004.

Catuneanu, O., W. E. Galloway, Ch. G. S. T. C. Kendall, A. D. Miall, H. W. Posamentier, A. Strasser, and M. E. Tucker (2011), Sequence Stratigraphy: Methodology and Nomenclature, *Newsletters on Stratigraphy*, *44*(3), 173–245, https://doi.org/10.1127/0078-0421/2011/0011.

Choquette, Ph. W., and N. P. James (1987), Diagenesis #12. Diagenesis in Limestones – 3. The Deep Burial Environment, *Geoscience Canada*, *14*(1), 3–35.

Choquette, Ph. W., and L. C. Pray (1970), Geologic Nomenclature and Classification of Porosity in Sedimentary Carbonates, *AAPG Bulletin*, *54*, 207–250.

Christie-Blick, N. (1991), Onlap, offlap, and the origin of unconformity-bounded depositional sequences, *Marine Geology*, *97*(1–2), 35–56, https://doi.org/10.1016/0025-3227(91)90018-Y.

Claes, S., F. H. Nader, and S. Youssef (2018), Coupled experimental/numerical workflow for assessing quantitative diagenesis and dynamic porosity/permeability evolution in calcite-cemented sandstone reservoir rocks, *Oil & Gas Science and Technology - Revue d'IFP Energies nouvelles*, *73*, 36, https://doi.org/10.2516/ogst/2018027.

Coniglio, M., R. Frizzell, and B. R. Pratt (2004), Reef-capping laminites in the Upper Silurian carbonate-to-evaporite transition, Michigan Basin, south-western Ontario, *Sedimentology*, *51*(3), 653–668, https://doi.org/10.1111/j.1365-3091.2004.00641.x.

Dehghanian, M. S., K. Khosrotehrani, M. Afghah, and F. Keshani (2012), Microfacies Study of Asmari Formation in the Northwest and Southeast of Shiraz, Iran, *Advances in Environmental Biology*, *6*(2), 556–563.

Dehghanian, M. S., B. Asgari Pirbalouti, and H. R. Masoumi (2013), Oligocene-Miocene Microfacies Study of Asmari Formation (NWSE of Shiraz, Iran), *Iranian Journal of Earth Sciences*, *5*, 66–73.

Dickson, J. A. D. (1978), Neomorphism and recrystallization, in *Sedimentology. Encyclopedia of Earth Science*, pp. 753–757, Springer Berlin Heidelberg, https://doi.org/10.1007/3-540-31079-7_143.

Dunham, R. J. (1962), Classification of Carbonate Rocks According to Depositional Texture, in *Classification of Carbonate Rocks-A Symposium*, pp. 108–121, American Association of Petroleum Geologists.

Ehrenberg, S. N., N. A. H. Pickard, G. V. Laursen, S. Monibi, Z. K. Mossadegh, T. A. Svånå, A. A. M. Aqrawi, J. M. McArthur, and M. F. Thirlwall (2007), Strontium isotope stratigraphy of the Asmari Formation (Oligocene-Lower Miocene), SW Iran, *Journal of Petroleum Geology*, *30*(2), 107–128, https://doi.org/10.1111/j.1747-5457.2007.00107.x.

El-Saiy, A. K., and B. R. Jordan (2007), Diagenetic aspects of tertiary carbonates west of the Northern Oman Mountains, United Arab Emirates, *Journal of Asian Earth Sciences*, *31*(1), 35–43, https://doi.org/10.1016/j.jseaes.2007.03.004.

Flügel, E. (2010), *Microfacies of Carbonate Rocks: Analysis, Interpretation and Application*, 984 pp., Springer Berlin Heidelberg, https://doi.org/10.1007/978-3-642-03796-2.

Garcia-Pichel, F. (2006), Plausible mechanisms for the boring on carbonates by microbial phototrophs, *Sedimentary Geology*, *185*(3–4), 205–213, https://doi.org/10.1016/j.sedgeo.2005.12.013.

Geert, K., A. M. Afifi, S. A. Al-Hajri, and H. J. Droste (2001), Paleozoic Stratigraphy and Hydrocarbon Habitat of the Arabian Plate, *GeoArabia*, *6*(3), 407–442, https://doi.org/10.2113/geoarabia0603407.

Grabowski, G. J., and I. O. Norton (1995), Tectonic controls on the stratigraphic architecture and hydrocarbon systems of the Arabian Plate, in *SEG Technical Program Expanded Abstracts 1995*, pp. 413–430, Society of Exploration Geophysicists, https://doi.org/10.1190/1.1887546.

Haidari, Kh., A. Amini, M. AleAli, A. Solgi, and J. Jafari (2020), Distribution pattern of Ahwaz sandstone and Kalhur evaporite members of Asmari Formation in Dezful Embayment and Abadan plain, a basis for stratigraphic traps studies, *Geopersia*, *10*(1), 53–63, https://doi.org/10.22059/geope.2019.275999.648463.

Hakimzadeh, S., and A. Seyrafian (2008), Late oligocene-early miocene benthic foraminifera and biostratigraphy of the Asmari Formation south Yasuj, north-central Zagros basin, Iran, *Carbonates and Evaporites*, *23*(1), 1–10, https://doi.org/10.1007/BF03176247.

Haq, B. U., and V. Al-Qahtani (2005), Phanerozoic cycles of sea-level change on the Arabian Platform, *GeoArabia*, *10*(2), 36.

Haq, B. U., and V. Eysinga (1998), A geological time table.

Haq, B. U., J. Hardenbol, and P. R. Vail (1987), Chronology of Fluctuating Sea Levels Since the Triassic, *Science*, *235*(4793), 1156–1167, https://doi.org/10.1126/science.235.4793.1156.

Haq, B. U., J. Hardenbol, and P. R. Vail (1988), *Mesozoic and Cenozoic chronostratigraphy and cycles of sea-level change, in Sea-Level Changes - An Integrated Approach*, pp. 71–108, SEPM (Society for Sedimentary Geology), https://doi.org/10.2110/pec.88.01.0071.

Heckel, Ph. H. (1983), Diagenetic Model For Carbonate Rocks In Midcontinent Pennsylvanian Eustatic Cyclothems, *SEPM Journal of Sedimentary Research*, *53*, https://doi.org/10.1306/212f82b0-2b24-11d7-8648000102c1865d.

Hosa, A., and R. Wood (2020), Order of diagenetic events controls evolution of porosity and permeability in carbonates, *Sedimentology*, *67*(6), 3042–3054, https://doi.org/10.1111/sed.12733.

Hosseinpour, M., Z. Maleki, and M. leali (2017), Evaluation of Hydrocarbon Potential in the Jahrom Area, Interior Fars, Zagros, *Open Journal of Geology*, *07*(03), 429–442, https://doi.org/10.4236/ojg.2017.73029.

Hosseinpour, M., M. Arian, Z. Maleki, and M. Ghorashi (2019), Fractal analysis of the effect of the Nezamabad fault on the lineaments related to fold: A case study of the Khaftar anticline, Zagros, Iran, *Tectonics*, *10*, 1–14.

Hughes, G. W., and Z. R. Beydoun (1992), The Red Sea-Gulf of Aden: biostratigraphy, lithostratigraphy and palaeoenvironments, *Journal of Petroleum Geology*, *15*(s3), 135–156, https://doi.org/10.1111/j.1747-5457.1992.tb00959.x.

Hughes, G. W., and J. Filatoff (1995), New biostratigraphic constraints on Saudi Arabian Red Sea pre- and syn-rift sequences, in *Middle East petroleum geosciences*, pp. 517–528, Gulf Petrolink.

Hughes, G. W., and R. S. Johnson (2005), Lithostratigraphy of the Red Sea Region, *GeoArabia*, *10*(3), 49–126, https://doi.org/10.2113/geoarabia100349.

Hughes, G. W., O. Varol, and Z. R. Beydoun (1991), Evidence for Middle Oligocene rifting of the Gulf of Aden and for Late Oligocene rifting of the southern Red Sea, *Marine and Petroleum Geology*, *8*(3), 354–358, https://doi.org/10.1016/0264-8172(91)90088-I.

Hughes, G. W., S. Abdine, and M. H. Girgis (1992), Miocene biofacies development and geological history of the Gulf of Suez, Egypt, *Marine and Petroleum Geology*, *9*(1), 2–28, https://doi.org/10.1016/0264-8172(92)90002-V.

Hughes, G. W., D. J. Grainger, A.-J. Abu-Bshait, and M. J. Abdul-Rahman (1999), Lithostratigraphy and Depositional History of Part of the Midyan Region, Northwestern Saudi Arabia, *GeoArabia*, *4*(4), 503–542, https://doi.org/10.2113/geoarabia0404503.

Hunt, D., and M. E. Tucker (1992), Stranded parasequences and the forced regressive wedge systems tract: deposition during base-level'fall, *Sedimentary Geology*, *81*(1–2), 1–9, https://doi.org/10.1016/0037-0738(92)90052-S.

Hunt, D., and M. E. Tucker (1995), Stranded parasequences and the forced regressive wedge systems tract: deposition during base-level fall-reply, *Sedimentary Geology*, *95*(1–2), 147–160, https://doi.org/10.1016/0037-0738(94)00123-C.

Karami, S., V. Ahmadi, H. Sarooe, and M. Bahrami (2020), Facies analysis and depositional environment of the Oligocene-Miocene Asmari Formation, in Interior Fars (Zagros Basin, Iran), *Carbonates and Evaporites*, *35*(3), https://doi.org/10.1007/s13146-020-00621-5.

Koop, W. J., and R. Stoneley (1982), Subsidence history of the Middle East Zagros basin, Permian to recent, *Philosophical Transactions A*, *305*, 149–168, https://doi.org/10.1098/rsta.1982.0031.

Lakshtanov, L. Z., L. Z. Okhrimenko, O. N. Karaseva, and S. L. S. Stipp (2018), Limits on Calcite and Chalk Recrystallization, *Crystal Growth & Design*, *18*(8), 4536–4543, https://doi.org/10.1021/acs.cgd.8b00537.

Langer, M. R., and L. Hottinger (2000), Biogeography of selected "larger" foraminifera, *Micropaleontology*, *46*, 105–106.

Laursen, G. V., S. Monibi, T. L. Allan, N. A. H. Pickard, A. Hosseiney, et al. (2009), The Asmari Formation Revisited: Changed Stratigraphic Allocation and New Biozonation, in *1st International Petroleum Conference and Exhibition Shiraz 2009*, EAGE Publications BV, https://doi.org/10.3997/2214-4609.20145919.

Lees, G. M. (1933), Reservoir Rocks of Persian Oil Fields, *AAPG Bulletin*, *17*, 224–240, https://doi.org/10.1306/3D932B32-16B1-11D7-8645000102C1865D.

Llinas, J. C. (2002), Diagenetic history of the Upper Jurassic Smackover Formation and its effects on reservoir properties: Vocation Field, Manila SubBasin, Eastern Gulf Coastal Plain, *Gulf Coast Association of Geological Societies Transactions*, *52*, 631–644.

Longman, M. W. (1980), Carbonate Diagenetic Textures from Nearsurface Diagenetic Environments, *AAPG Bulletin*, *64*, 461–487, https://doi.org/10.1306/2F918A63-16CE-11D7-8645000102C1865D.

Madden, R. H. C., M. E. J. Wilson, M. Mihaljević, J. M. Pandolfi, and K. Welsh (2017), Unravelling the depositional origins and diagenetic alteration of carbonate breccias, *Sedimentary Geology*, *357*, 33–52, https://doi.org/10.1016/j.sedgeo.2017.05.002.

Maghfouri, S., E. Rastad, G. Borg, M. R. Hosseinzadeh, M. Movahednia, A. Mahdavi, and F. Mousivand (2020), Metallogeny and temporal-spatial distribution of sediment-hosted stratabound copper (SSC-type) deposits in Iran; implications for future exploration, *Ore Geology Reviews*, *127*, 103,834, https://doi.org/10.1016/j.oregeorev.2020.103834.

Mahmoodabadi, R. M. (2014), Petrography, Sedimentary Environments and Sequence Stratigraphy of Asmari Formation in Central Fars, Zagros, SW (Iran), *Open Journal of Geology*, *04*(12), 665–679, https://doi.org/10.4236/ojg.2014.412050.

Maleki, Z., M. Arian, A. Solgi, and M. A. Ganjavian (2014), The Elements of Fold Style Analysis in the Khaftar Anticline, Zagros, Iran, *Open Journal of Geology*, *04*(03), 79–92, https://doi.org/10.4236/ojg.2014.43008.

Maleki, Z., M. Arian, and A. Solgi (2015), Folding pattern in the Fars province, Zagros folded belt: case study on the Karbasi and Khaftar anticlines, interior Fars, Iran, *Solid Earth Discussions*, *7*(3), 2347–2379, https://doi.org/10.5194/sed-7-2347-2015.

McLaughlin, P. P. (2005), Sequence stratigraphy, in *Encyclopedia of Geology*, pp. 159–173, Elsevier, https://doi.org/10.1016/B0-12-369396-9/00043-5.

Menke, H. P., M. G. Andrew, M. J. Blunt, and B. Bijeljic (2016), Reservoir condition imaging of reactive transport in heterogeneous carbonates using fast synchrotron tomography - Effect of initial pore structure and flow conditions, *Chemical Geology*, *428*, 15–26, https://doi.org/10.1016/j.chemgeo.2016.02.030.

Menke, H. P., B. Bijeljic, and M. J. Blunt (2017), Dynamic reservoir-condition microtomography of reactive transport in complex carbonates: Effect of initial pore structure and initial brine pH, *Geochimica et Cosmochimica Acta*, *204*, 267–285, https://doi.org/10.1016/j.gca.2017.01.053.

Morse, J. W., and F. T. Mackenzie (1990), Early non-marine diagenesis of sedimentary, in *Developments in Sedimentology*, chap. 7, pp. 277–371, Elsevier, https://doi.org/10.1016/s0070-4571(08)70336-4.

Nadjafi, M., A. Mahboubi, R. Moussavi-Harami, and R. Mirzaee (2004), Depositional History and Sequence Stratigraphy of Outcropping Tertiary Carbonates in the Jahrum and Asmari Formations, Shiraz Area (SW Iran), *Journal of Petroleum Geology*, *27*(2), 179–190, https://doi.org/10.1111/j.1747-5457.2004.tb00052.x.

Ogg, J. G., G. M. Ogg, and F. M. Gradstein (2016), *A concise geologic time scale*, 221 pp., Elsevier, https://doi.org/10.1016/c2009-0-64442-1.

Patzkowsky, M. E., and S. M. Holland (2012), *Stratigraphic paleobiology: Understanding the distribution of fossil taxa in time and space*, 221 pp., The University of Chicago Press.

Player, R. A. (1969), The Hormuz salt plugs of southern Iran, phdthesis.

Plint, A. G. (1990), An allostratigraphic correlation of the Muskiki and Marshybank formations (Coniacian-Santonian) in the Foothills and subsurface of the Alberta Basin, *Bulletin of Canadian Petroleum Geology*, *38*, 288–306, https://doi.org/10.35767/gscpgbull.38.3.288.

Plint, A. G., and D. Nummedal (2000), The falling stage systems tract: recognition and importance in sequence stratigraphic analysis, *Geological Society, London, Special Publications*, *172*(1), 1–17, https://doi.org/10.1144/GSL.SP.2000.172.01.01.

Posamentier, H. W., and M. T. Jervey (1988), Sequence stratigraphy; implications for facies models and reservoir occurrence, *CSPG Reservoir*, *15*(6), 1–2.

Posamentier, H. W., and P. R. Vail (1988), Sequence stratigraphy; sequences and systems tract development, *Memoir Canadian Society of Petroleum Geologists*, *15*, 571–572.

Poursoltani, M. R., and M. Harati-Sabzvar (2019), Porosity evolution and diagenetic history of the upper Jurassic Mozduran Formation, eastern Kopet-Dagh Basin, NE Iran, *Iranian Journal of Earth Sciences*, *11*(2), 141–159.

Rahmani, A., H. Vaziri-Moghaddam, A. Taheri, and A. Ghabeishavi (2009), A model for the paleoenvironmental distribution of larger foraminifera of Oligocene-Miocene carbonate rocks at Khaviz Anticline, Zagros Basin, SW Iran, *Historical Biology*, *21*(3–4), 215–227, https://doi.org/10.1080/08912960903461296.

Razavi Pash, R., K. Sarkarinejad, S. Sherkati, and H. Motamedi (2021), Analogue model of the Bala Rud Fault, Zagros: an oblique basement ramp in a fold-and-thrust belt, *International Journal of Earth Sciences*, *110*(2), 741–755, https://doi.org/10.1007/s00531-021-01987-0.

Reid, R. P., and I. G. Macintyre (1998), Carbonate recrystallization in shallow marine environments: a widespread diagenetic process forming micritized grains, *Journal of Sedimentary Research*, *68*(5), 928–946, https://doi.org/10.2110/jsr.68.928.

Richardson, R. K. (1924), The geology and oil measures of southwest Persia, *Journal of the Institute of Petroleum Technology*, *1*, 256–283.

Salih, N., H. Mansurbeg, K. Kolo, and A. Préat (2019), Hydrothermal Carbonate Mineralization, Calcretization, and Microbial Diagenesis Associated with Multiple Sedimentary Phases in the Upper Cretaceous Bekhme Formation, Kurdistan Region-Iraq, *Geosciences*, *9*(11), 459, https://doi.org/10.3390/geosciences9110459.

Scholle, P. A., and R. B. Halley (1985), Burial diagenesis: out of sight, out of mind!, in *SEPM Special Publication*, vol. 36, pp. 309–334, Society of Economic Paleontologists and Mineralogists.

Scholle, P. A., and D. S. Ulmer-Scholle (2003), *A Color Guide to the Petrography of Carbonate Rocks: Grains, textures, porosity, diagenesis*, American Association of Petroleum Geologists, https://doi.org/10.1306/M77973.

Sepehr, M., and J. W. Cosgrove (2004), Structural framework of the Zagros FoldThrust Belt, Iran, *Marine and Petroleum Geology*, *21*(7), 829–843, https://doi.org/10.1016/j.marpetgeo.2003.07.006.

Sepehr, M., and J. W. Cosgrove (2005), Role of the Kazerun Fault Zone in the formation and deformation of the Zagros Fold-Thrust Belt, Iran, *Tectonics*, *24*(5), https://doi.org/10.1029/2004TC001725.

Sepehr, M., and J. W. Cosgrove (2007), The role of major fault zones in controlling the geometry and spatial organization of structures in the Zagros Fold-Thrust Belt, *Geological Society, London, Special Publications*, *272*(1), 419–436, https://doi.org/10.1144/GSL.SP.2007.272.01.21.

Setudehnia, A. (1978), The Mesozoic sequence in south-west Iran and adjacent areas, *Journal of Petroleum Geology*, *1*(1), 3–42, https://doi.org/10.1111/j.1747-5457.1978.tb00599.x.

Seyrafian, A., and A. Hamedani (2003), Microfacies and paleoenvironmental interpretation of the lower Asmari Formation (Oligocene), North-Central Zagros Basin, Iran, *Neues Jahrbuch für Geologie und Paläontologie - Monatshefte*, *2003*(3), 164–174, https://doi.org/10.1127/njgpm/2003/2003/164.

Sharland, P. R., R. Archer, and D. M. Casey (2001), Maximum flooding surfaces, in *Arabian Plate Sequence Stratigraphy*, chap. 4, pp. 261–278, GeoArabia.

Sherman, C. E., C. H. Fletcher, and K. H. Rubin (1999), Marine and meteoric diagenesis of Pleistocene carbonates from a nearshore submarine terrace, Oahu, Hawaii, *Journal of Sedimentary Research*, *69*(5), 1083–1097, https://doi.org/10.2110/jsr.69.1083.

Shogenova, A., and A. Kleesment (2006), Diagenetic influences on iron-bearing minerals in Devonian carbonate and siliciclastic rocks of Estonia, *Proceedings of the Estonian Academy of Sciences. Geology*, *55*(4), 269, https://doi.org/10.3176/geol.2006.4.02.

Sibley, D., and J. Gregg (1987), Classification of Dolomite Rock Texture, *Journal of sedimentary petrology*, *57*, 967–975.

Sooltanian, N., A. Seyrafian, and H. Vaziri-Moghaddam (2011), Biostratigraphy and paleo-ecological implications in microfacies of the Asmari Formation (Oligocene), Naura anticline (Interior Fars of the Zagros Basin), Iran, *Carbonates and Evaporites*, *26*(2), 167–180, https://doi.org/10.1007/s13146-011-0053-6.

Talbot, C. J., and M. Alavi (1996), The past of a future syntaxis across the Zagros, *Geological Society, London, Special Publications*, *100*(1), 89–109, https://doi.org/10.1144/GSL.SP.1996.100.01.08.

Tucker, M. E., and V. P. Wright (1990), *Carbonate Sedimentology*, Wiley, https://doi.org/10.1002/9781444314175.

Tucker, R. D., P. H. Osberg, and H. N. Berry (2001), The geology of a part of Acadia and the nature of the Acadian orogeny across Central and Eastern Maine, *American Journal of Science*, *301*(3), 205–260, https://doi.org/10.2475/ajs.301.3.205.

Vail, P. R., and R. M. Mitchum (1977), Seismic Stratigraphy and Global Changes of Sea Level, Part 1: Overview, in *Seismic Stratigraphy - Applications to Hydrocarbon Exploration*, vol. 26, pp. 51–52, American Association of Petroleum Geologists, https://doi.org/10.1306/M26490C3.

Vail, P. R., R. M. Mitchum, and S. Thompson (1977a), Seismic Stratigraphy and Global Changes of Sea Level, Part 4: Global Cycles of Relative Changes of Sea Level, in *Seismic Stratigraphy - Applications to Hydrocarbon Exploration*, American Association of Petroleum Geologists, https://doi.org/10.1306/M26490C6.

Vail, P. R., R. M. Mitchum, and S. Thompson (1977b), Seismic Stratigraphy and Global Changes of Sea Level, Part 3: Relative Changes of Sea Level from Coastal Onlap, in *Seismic Stratigraphy - Applications to Hydrocarbon Exploration*, American Association of Petroleum Geologists, https://doi.org/10.1306/M26490C5.

Vail, P. R., R. G. Todd, and J. B. Sangree (1977c), Seismic Stratigraphy and Global Changes of Sea Level, Part 5: Chronostratigraphic Significance of Seismic Reflections, in *Seismic Stratigraphy - Applications to Hydrocarbon Exploration*, American Association of Petroleum Geologists, https://doi.org/10.1306/M26490C7.

van Buchem, F. S. P., T. L. Allan, G. V. Laursen, M. Lotfpour, et al. (2010), Regional stratigraphic architecture and reservoir types of the Oligo-Miocene deposits in the Dezful Embayment (Asmari and Pabdeh Formations) SW Iran, *Geological Society, London, Special Publications*, *329*(1), 219–263, https://doi.org/10.1144/SP329.10.

van Houten, F. B. (1973), Origin of Red Beds A Review-1961-1972, *Annual Review of Earth and Planetary Sciences*, *1*(1), 39–61, https://doi.org/10.1146/annurev.ea.01.050173.000351.

van Wagoner, J. C., H. W. Posamentier, R. M. Mitchum, P. R. Vail, J. F. Sarg, T. S. Loutit, and J. Hardenbol (1988), An overview of the fundamentals of sequence stratigraphy and key definitions, in *Sea-Level Changes*, pp. 39–45, SEPM (Society for Sedimentary Geology), https://doi.org/10.2110/pec.88.01.0039.

van Wagoner, J. C., R. M. Mitchum, K. M. Campion, and V. D. Rahmanian (1990), *Siliciclastic Sequence Stratigraphy in Well Logs, Cores, and Outcrops: Concepts for High-Resolution Correlation of Time and Facies*, American Association of Petroleum Geologists, https://doi.org/10.1306/Mth7510.

van Wagoner, J. C., D. Nummedal, C. R. Jones, D. R. Taylor, D. C. Jennette, and G. W. Riley (1991), *Sequence Stratigraphy Applications to Shelf Sandstone Reservoirs*, American Association of Petroleum Geologists.

Vaziri-Moghaddam, H., M. Kimiagari, and A. Taheri (2005), Depositional environment and sequence stratigraphy of the Oligo-Miocene Asmari Formation in SW Iran, *Facies*, *52*(1), 41–51, https://doi.org/10.1007/s10347-005-0018-0.

Vaziri-Moghaddam, H., A. Seyrafian, A. Taheri, and H. Motiei (2010), Oligocene-Miocene ramp system (Asmari Formation) in the NW of the Zagros basin, Iran: Microfacies, paleoenvironment and depositional sequence, *Revista Mexicana de Ciencias Geológicas*, *27*(1), 56–71.

Vincent, B., L. Emmanuel, P. Houel, and J.-P. Loreau (2007), Geodynamic control on carbonate diagenesis: Petrographic and isotopic investigation of the Upper Jurassic formations of the Paris Basin (France), *Sedimentary Geology*, *197*(3–4), 267–289, https://doi.org/10.1016/j.sedgeo.2006.10.008.

Warren, J. K. (2010), Evaporites through time: Tectonic, climatic and eustatic controls in marine and nonmarine deposits, *Earth-Science Reviews*, *98*(3–4), 217–268, https://doi.org/10.1016/j.earscirev.2009.11.004.

Wilson, J. L. (1975), *Carbonate Facies in Geologic History*, Springer New York, https://doi.org/10.1007/978-1-4612-6383-8.

Wilson, M. E. J., and M. J. Evans (2002), Sedimentology and diagenesis of Tertiary carbonates on the Mangkalihat Peninsula, Borneo: implications for subsurface reservoir quality, *Marine and Petroleum Geology*, *19*(7), 873–900, https://doi.org/10.1016/S0264-8172(02)00085-5.

Yarem Taghloo Sohrabi, M., B. Soleimani, V. Ahmadi, D. Jahani, and N. Kohansal Ghadimvand (2019), Investigation of Sequential Stratigraphy, Microfacies, Sedimentary Environment and Diagenesis Processes of Asmari Formation in Interior Fars Areas, Iran (Farashband, Sarvestan, Kalestan), *Environment and Ecology*, *37*(4B), 1546–1560.